ELSEVIER

Biophysical Chemistry 112 (2004) 257–266

Biophysical Chemistry

www.elsevier.com/locate/bpc

Do the isolated fibrinogen αC-domains form ordered oligomers?

Galina Tsurupa[a], Yury Veklich[b], Roy Hantgan[c], Alexey M. Belkin[a], John W. Weisel[b], Leonid Medved[a,*]

[a]*Biochemistry Department, Jerome H. Holland Laboratory for the Biomedical Sciences, American Red Cross, 15601 Crabbs Branch Way, Rockville, MD 20855, United States*

[b]*Department of Cell and Developmental Biology, University of Pennsylvania School of Medicine, Philadelphia, PA 19104, United States*

[c]*Wake Forest University School of Medicine, Winston-Salem, NC 27157, United States*

Received 5 June 2004; accepted 1 July 2004
Available online 27 August 2004

Abstract

Previous electron microscopy (EM) studies revealed that the proteolytically prepared, truncated, bovine fibrinogen αC-domain (Aα223-539 fragment) upon transfer from acidic to neutral pH formed ordered oligomers which could mimic α polymers of cross-linked fibrin. In this study, we demonstrated that although its recombinant analog, bAα224-538, as well as the full-length version of the αC-domain (bAα224-568), upon similar treatment also formed oligomers with ordered structure, both were monomeric when kept in neutral pH buffer. To search further for conditions for their oligomerization, we treated bAα224-568 with factor XIIIa, purified the cross-linked soluble fraction, and confirmed that it consisted of oligomers. Similar cross-linked oligomers were obtained with the recombinant human αC-domain (residues Aα221-610). In a cell adhesion assay, the adhesion of human umbilical vein endothelial cells (HUVEC) to the αC-domains substantially increased upon oligomerization. These results demonstrate that the recombinant αC-domains can form stable oligomers which may mimic properties of the αC-domains in cross-linked fibrin.

Keywords: Fibrinogen; αC-domains; Aggregation; Electron microscopy; Ultracentrifugation; Light scattering

1. Introduction

Fibrinogen is a multidomain plasma protein that plays a prominent role in hemostasis and participates in a number of other physiological and pathological processes through interaction with various proteins and cell types. Such a multifunctional character is connected with the presence of multiple interaction sites, which reside in numerous fibrinogen domains. Some of these domains are critical for fibrin assembly while others are involved in its regulation and are responsible for the subsequent contribution of fibrin to modulation of fibrinolysis, the inflammatory response, angiogenesis and wound healing. Among them are the αC-domains, which themselves contain multiple binding sites and seem to be involved in modulation of a number of fibrin(ogen) activities. They not only contribute to fibrin assembly [1–4] but also contain binding sites for tPA and plasminogen, and cross-linking sites for α_2-antiplasmin [5,6], which play a prominent role in regulation of fibrinolysis. As a result, the molecular defects in the αC-domains of several congenitally abnormal fibrinogens cause disfibrinogenemia associated with defective thrombolysis [7,8]. The αC-domains control activation of factor XIII [9], and become cross-linked by it to α_2-antiplasmin, PAI-2, von Willebrand factor, thrombospondin, fibronectin, and some other proteins [6,10–13]. They are also involved in interactions with a number of cell types via their Aα572-574 RGD sequence and via bound fibronectin [14–16].

The αC-domains are formed by the COOH terminal portions of two fibrinogen Aα chains (residues 221–610), which are easily removed upon proteolysis [4]. Although the αC-domains (as well as the NH_2-terminal portions of the Bβ chains) are the only regions in fibrinogen whose 3D

* Corresponding author. Tel.: +1 301 738 0719; fax: +1 301 738 0740.
E-mail address: medvedL@usa.redcross.org (L. Medved).

0301-4622/$ - see front matter © 2004 Elsevier B.V. All rights reserved.
doi:10.1016/j.bpc.2004.07.028

structure was not established [17], previous and recent studies have clarified their structural organization. Based on the electron microscopy and differential scanning calorimetry data, it was hypothesized that each αC-domain consists of a compact COOH-terminal region attached to the bulk of the molecule via a flexible NH_2-terminal connector [18–21]. Recent experiments with the recombinant fragments corresponding to the αC-domain and its NH_2- and COOH-terminal halves confirmed that the αC-domain indeed consists of two structurally distinct regions, a flexible connector including residues 221–391 and an independently folded, compact portion including residues 392–610[1] [22].

Numerous data revealed that in fibrinogen the αC-domains interact intramolecularly with each other and probably with the central region E, while in fibrin they are covalently cross-linked by factor XIIIa intermolecularly to form high molecular mass α polymers (reviewed in Ref. [4]). Arrangement of the αC-domains into α polymers seems to change dramatically their functional properties. For example, their tPA- and plasminogen-binding sites, as well as apolipoprotein(a)- and fibronectin-binding sites, are cryptic in fibrinogen and become available in fibrin [5,23,24] suggesting that the αC-domains may undergo conformational changes upon α polymer formation resulting in exposure of their multiple interaction sites. Another alternative is that these binding sites are created through the unique juxtaposition of regions of two or more αC-domains as a result of polymerization. It was hypothesized that formation of α polymers is a result of the "intra-to-intermolecular switch". Namely, upon fibrin assembly the αC-domains switch from intra- to intermolecular interactions to form α polymers; the flexible connector provides mobility to the compact αC-domains during such a "switch" and factor XIIIa reinforces these polymers by intermolecular cross-linking [4]. The cross-linking occurs through a number of reactive Gln and Lys residues which are located in the different parts of the αC-domains. Most of the reactive lysine residues were localized in the compact part ("head") while the connector region ("tail") contains mainly reactive glutamyls [25]. Although this fact suggests that the αC-domains in α polymers could be arranged in a "head-to-tail" manner, the exact mechanism of α polymer formation remains to be established.

Investigation of the mechanism of α polymer formation and its functions in fibrin is complicated by the complexity of fibrin structure and the presence of multiple domains some of which could duplicate activities of the αC-domains, for example their interaction with tPA and plasminogen. Previous electron microscopy (EM^2) studies revealed that a truncated αC-domain fragment isolated from a plasmin digest of bovine fibrinogen can form oligomers with ordered structure [26]. That finding supported the "intra-to-intermolecular switch" hypothesis and suggested that oligomerization of the isolated αC-fragment could mimic formation of α polymers in fibrin. However, preparation of such a fragment, as well as its counterpart from human fibrinogen, was complicated by a very low yield due to high susceptibility of the αC-domains to proteolysis [26,27]. In addition, only truncated fragments missing the COOH-terminal regions were recovered from plasmin digests of both bovine and human fibrinogens [26,27]. To overcome these problems, we expressed bovine and human αC-domains and their variants by recombinant techniques [22]. The major goals of this study were to test the ability of the recombinant αC-domains to self-aggregate and to search for appropriate models mimicking structural and functional features of the fibrin αC-domains.

2. Experimental procedures

2.1. Recombinant αC-domain variants

A truncated variant of the bovine αC-domain, bAα224-538, was expressed in *Escherichia coli* using the pET-20b expression vector containing sequence for the full-length bovine αC-domain [22] and the following primers, 5′-AGAGACATATGCAGCTCCAAGAGGCCCC-3′ (forward) and 5′-AGAGAAAGCTTCTAGGCAGGACGAGCTTTAGTATG-3′ (reverse). The forward primer incorporated the *Nde*I restriction site immediately before the coding region; the final three bases of the *Nde*I site, ATG, code for the fMet residue that initiate translation. The reverse primer included a TAA stop codon immediately after the coding segment, following by a *Hin*dIII site. The amplified cDNA fragments were purified by electrophoresis in agarose gel, digested with *Nde*I and *Hin*dIII restriction enzymes, and ligated into the pET-20b expression vector (Novagen). The resulting plasmids were used for transformation of DH5α and then B834(DE3) pLysS *E. coli* host cells. The cDNA fragment was sequenced in both directions to confirm the integrity of the coding sequences. The bAα224-538 fragment was found in inclusion bodies from which it was purified by the procedure described earlier [22].

The recombinant bovine fibrinogen bAα224-568 fragment (full-length αC-domain) and its sub-fragments, bAα224-373 and bAα374-568, and the recombinant full-length human fibrinogen αC-domain (hAα221-610) and its sub-fragments, hAα221-391 and hAα392-610, were produced in *E. coli* as described earlier [5,22].

All fragments, including bAα224-538, were refolded according to the procedures described in Ref. [22], passed through a Superdex 200 HR column (Pharmacia) equilibrated with 20 mM Tris buffer, pH 7.5, with 150 mM NaCl, 0.1 mM PMSF, 0.02% NaN_3 (TBS) to remove unfolded fractions, concentrated to 1.5–2.0 mg/ml, and kept at 4 °C. To prepare

[1] Although it is more reasonable to refer to the compact part as the αC-domain and the flexible part as the αC-connector as suggested earlier [22], in this paper, we use traditional nomenclature according to which the αC-domain includes both the compact part and the connector [4].

[2] EM, electron microscopy, TBS, 20 mM Tris–HCl, pH 7.5, 150 mM NaCl, 0.1 mM PMSF, 0.02% NaN_3; GBS, 20 mM Gly buffer, pH 3.5, with 150 mM NaCl; HUVEC, human umbilical vein endothelial cells.

samples in acidic buffer, the selected fragments were transferred into ice-chilled 20 mM Gly buffer, pH 3.5, containing 150 mM NaCl (GBS) by rapid 30-fold dilution upon stirring, concentrated to 1.5–2.0 mg/ml, and kept at 4 °C.

2.2. Fluorescence study

Fluorescence measurements of thermal-induced unfolding of the αC-domain variants were performed in an SLM 8000-C fluorometer by monitoring the ratio of the intensity at 370 nm to that at 330 nm with excitation at 280 nm. Temperature was controlled with a circulating water bath programmed to raise the temperature at 1 °C/min. Protein concentrations determined spectrophotometrically as described in Ref. [22] were 0.02–0.1 mg/ml.

2.3. Turbidity measurements

To test the ability of the αC-domain variants to self-aggregate, each fragment was diluted 50-fold in a spectrophotometric cuvette containing TBS at room temperature and turbidity changes were monitored at 350 nm with an HP 8453 spectrophotometer. The final concentration of all fragments was about 0.04 mg/ml.

2.4. Transmission electron microscopy studies

Samples for electron microscopy were prepared by spraying a dilute solution of the recombinant fragments in a volatile buffer (50 mM ammonium formate, pH 7.4, or 0.125% acetic acid, pH 3.5) and 25–30% glycerol onto freshly cleaved mica and rotary shadowing with tungsten in a vacuum evaporator as previously described [26]. Specimens were examined in a Philips 400 electron microscope (FEI, Hillsboro, OR) at 80 kV and 60,000× magnification.

2.5. Size-exclusion chromatography

Analytical size-exclusion chromatography was used to determine apparent molecular masses of the αC-domain variants. FPLC and HPLC experiments were performed at a flow rate of 0.5 ml/min and room temperature using a 30×0.1 cm Superdex 200 HR column (Pharmacia) and a 30×0.78 cm TSK-Gel G3000SWxl column (TOSOH Bioscience LLC), respectively. Typically, 50 μl of each fragment at 2 mg/ml were loaded onto the column equilibrated with TBS followed elution with the same buffer. The elution was monitored by measuring the absorbance at 280 nm. To determine molecular masses of the recombinant fragments, both columns were calibrated with the gel filtration HMW and LMW calibration kits (Amersham).

2.6. Light scattering measurements

The apparent molecular masses of the αC-domain variants were determined using multi-angle light scattering technique. Typically, 50 μl of each fragment at 2 mg/ml were loaded onto the TSK-Gel G3000SWxl HPLC column which was followed in-line by a DAWN EOS light scattering detector (Wyatt Technologies) and an interferometric refractometer (Wyatt Technologies). Molecular masses of the fragments were calculated from a Zimm plots using ASTRA software (Wyatt Technologies). The change in refractive index as a function of protein concentration is approximately constant for proteins and a value of 0.185 ml/g was used [28].

2.7. Analytical ultracentrifugation

Samples for analytical ultracentrifugation were prepared by overnight dialysis of the selected fragments at 0.5–2.5 mg/ml versus TBS. Sedimentation velocity measurements were performed in a Beckman Optima XL-A analytical ultracentrifuge (Beckman Instruments, Palo Alto, CA) equipped with absorbance optics and an An60 Ti rotor, as previously described [29,30]. Sedimentation velocity data were collected with each αC-domain variant at 20 °C at a rotor speed of 45,000 rpm. Sedimentation velocity data were analyzed using both SVEDBERG (version 1.04) and DCDT+ (version 6.31) software (J. Philo, Thousand Oaks, CA) to obtain the weight-average sedimentation coefficient (S_w) and distribution of sedimenting species, $g(s^*)$, respectively [31,32]. All sedimentation coefficients have been corrected for solvent density and viscosity to obtain $S_{20,w}$ values.

2.8. Cross-linking with factor XIIIa

Cross-linking of the αC-domain variants with factor XIIIa was performed similarly to that described in Ref. [5]. The reaction mixture contained 1 mg/ml of the αC-domain variants, 30 μg/ml factor XIII, and 1 NIH unit/ml α-thrombin in TBS with 10 mM Ca^{2+}. The mixture was incubated for 2 h at room temperature, centrifuged to remove nonsoluble material, and then fractionated by size-exclusion chromatography on a Superdex 200 HR column.

2.9. Cell adhesion assay

Tissue culture plastic wells were coated with the recombinant human αC-fragment (hAα221-610) or its FXIIIa-cross-linked oligomers, both at 20 μg/ml in TBS, for 12 h at 4 °C, and then blocked with 10 mg/ml bovine serum albumin (Calbiochem) in TBS. For adhesion studies, ^{35}S-labeled human umbilical vein endothelial cells (HUVEC) were detached by trypsinization and 10^5 cells per well were plated in serum-free DMEM (Gibco) for 20 min at 37 °C either without or in the presence of 250 μg/ml GRGDSP or GRGESP peptides (American Peptide, Sunny Valley, CA). Adherent cells were washed three times with PBS and lysed in 1% SDS. The bound radioactivity was counted in a Beckman LS 3801 scintillation counter and converted into the number of adherent cells by referring to the levels of ^{35}S incorporation/10^3 cells.

3. Results

Formation of ordered oligomers by the proteolytically prepared, truncated variant of the bovine fibrinogen αC-domain was previously observed by electron microscopy upon transferring this variant from acidic to neutral pH [26]. However, when the human fibrinogen αC-domain fragment was originally expressed in *E. coli* [25] and tested, we were unable to obtain similar oligomers (unpublished results). It was unclear whether such behavior of the recombinant fragment was connected with the difference in the properties of human and bovine αC-domains, or if it was a result of its possible unfolding at acidic pH. Therefore, in this study we first expressed the full-length bovine αC-domain, bAα224-568, and its truncated version, bAα224-538, corresponding to the previously described proteolytic bovine Aα223-539 fragment[3] [26] and tested their folding status, and then tested their ability to self-associate upon transferring from acidic to neutral pH.

3.1. Folding status of the recombinant αC-fragments

Both the bAα224-568 and bAα224-538 recombinant fragments were expressed in *E. coli* and purified and refolded by the procedures described earlier [22]. To check if these fragments preserve their structure at acidic pH, we studied their heat-induced unfolding by monitoring the ratio of fluorescence intensity at 370 nm to that at 330 nm as a measure of a spectral shift that accompanies unfolding. The refolded fragments kept at neutral pH in TBS were transferred to acidic pH by a quick 10–30-fold dilution with GBS, incubated for 30 min at 4 °C, and then heated. Alternatively, the refolded fragments kept at acidic pH in GBS were diluted 10–30-fold with the same buffer and heated. In both sets of experiments, the fragments exhibited sigmoidal denaturation transitions (Fig. 1, curves 1 and 2) indicating that they were folded at acidic pH. In control experiments, when the αC-domain sub-fragment bAα224-373 (connector region), which has no compact structure [22], was treated in a similar manner, no transition was observed, while the bAα374-568 sub-fragment, which is compact at neutral pH [22], also exhibited a sigmoidal transition at acidic pH (Fig. 1, curves 3 and 4). When the bAα224-568, bAα224-538 and bAα374-568 fragments were transferred from acidic GBS to neutral TBS by quick dilution, incubated for 30 min at 4 °C, and then heated, they again exhibited sigmoidal transitions (not shown), similar to those obtained earlier with the same fragments at neutral pH [22]. These experiments indicated that all fragments except the connector region preserved their compact structure at acidic pH and after transferring them from acidic to neutral pH.

[3] The previously isolated proteolytic bovine fibrinogen αC-fragment consisted of a mixture of three fragments, Aα223-539, Aα234-539 and Aα243-539 [2,22,26].

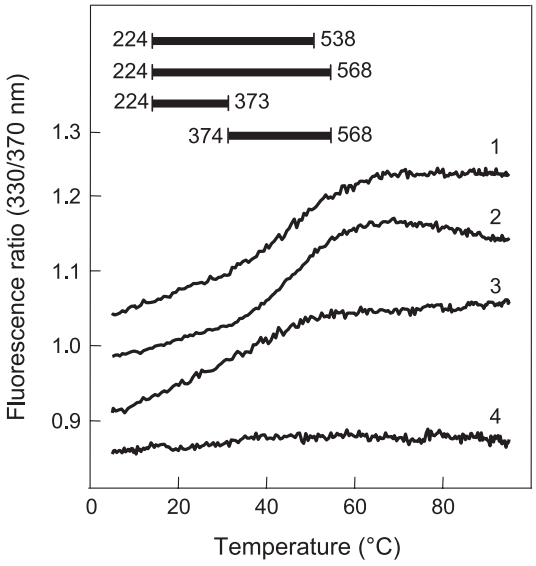

Fig. 1. Fluorescence-detected thermal denaturation of the recombinant bovine αC-domain and its truncated variants. Schematic representation of the studied fragments is given in the left upper corner. Curves 1, 2, 3 and 4 were obtained upon heating the bAα224-538, bAα224-568, bAα374-568, and bAα224-373 fragments, respectively, in acidic pH GBS (20 mM Gly buffer, pH 3.5, with 150 mM NaCl). All curves were arbitrarily shifted along the vertical axis to improve visibility.

3.2. Formation of oligomers by the recombinant αC-fragments

To check whether the truncated recombinant bovine αC-fragment, bAα224-538, is able to form oligomers similar to those observed with the proteolytically isolated bovine Aα223-539 fragment [26], we transferred it from acidic to neutral pH by quick dilution into TBS to final concentration 0.04 mg/ml and monitored turbidity at 350 nm. Time-dependent changes in turbidity were observed (Fig. 2, curve 1) suggesting the formation of aggregates. A similar result was obtained with the bAα224-568 fragment corresponding to the full-length bovine αC-domain (Fig. 2, curve 2). In control experiments, when the fragments corresponding to the connector and compact regions (bAα224-373 and bAα374-568, respectively) were treated in a similar manner, there were no changes in turbidity (Fig. 2, curves 3 and 4).

To further characterize these aggregates, we turned to electron microscopy. When the recombinant truncated αC-domain, bAα224-538, kept in acidic GBS was diluted with an acidic electron microscopy buffer (0.125% acetic acid, pH 3.5, containing 30% glycerol) to a final concentration of 1 μM, sprayed onto freshly cleaved mica, and shadowed with tungsten, only globular structures with a diameter of about 4 nm were found (Fig. 3A). These structures were similar to those observed earlier at acidic pH with the proteolytically prepared truncated bovine αC-fragment [26]; they correspond most probably to the monomeric αC-domain species. Such structures were also noted when the

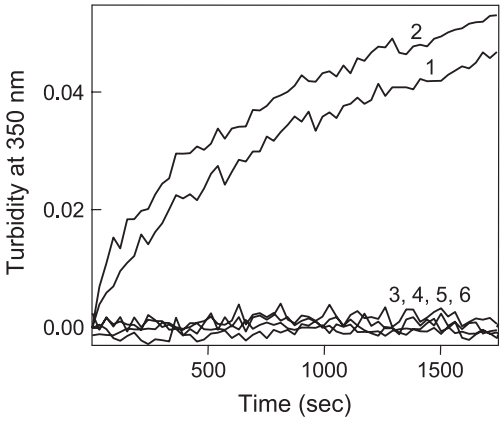

Fig. 2. Changes in turbidity at 350 nM observed after transfer of the recombinant bovine αC-domain and its truncated variants from acidic to neutral pH buffers. Curves 1, 2, 3 and 4 were obtained after transfer of the bAα224-538, bAα224-568, bAα374-568, and bAα224-373 fragments, respectively, from acidic pH GBS to neutral pH TBS (see text). Curves 5 and 6, which essentially coincide with curves 3 and 4, were obtained after dilution of the bAα224-538 and bAα224-568 fragments, kept in TBS, with the same buffer (see text).

fragment was transferred from acidic GBS to a neutral pH electron microscopy buffer (20 mM ammonium formate, pH 7.4, with 30% glycerol) by quick dilution to the same final concentration (Fig. 3B). In addition, we also observed numerous long linear branching arrays with a width of about 8 nm, similar to those described earlier for the proteolytic αC-fragment [26]. This is in agreement with the time-dependent increase in turbidity upon transferring this fragment from acidic to neutral pH (Fig. 2, curve 1). Similar results were obtained with the recombinant full-length bovine αC-fragment, bAα224-568 (Fig. 3D and E).

Altogether, the above experiments indicated that the recombinant bovine αC-domain variants, bAα224-568 and bAα224-538, like their proteolytic counterpart Aα223-539 fragment, are monomeric at acidic pH and that after their transfer to neutral pH buffer they form oligomers with ordered structure. They also suggested that these variants should form oligomers in another neutral pH buffer, TBS, in which the fragments are usually kept. However, when bAα224-568 and bAα224-538 kept in TBS were diluted with the neutral pH electron microscopy buffer and analyzed by EM, only globular structures similar to those in Fig. 3A were observed (Fig. 3C and F). There were also no changes in turbidity at 350 nM after their dilution with the same buffer (Fig. 2, curves 5 and 6). To clarify these unexpected observations, we tested the aggregation state of the αC-fragments in TBS by various methods.

3.3. Aggregation state of the recombinant αC-fragments in TBS

When the bAα224-568 and bAα224-538 fragments were analyzed by FPLC using a Superdex 200 HR column equilibrated with TBS and pre-calibrated with molecular mass standards, they both were eluted in a single peak. The apparent molecular masses of these fragments determined on the basis of their elution volumes and the elution volumes of the standards were 2.5–2.7-fold higher than those expected for the monomeric species (Table 1). Their sub-fragments, bAα224-373 and bAα374-568, were also eluted in a single peak and their apparent molecular masses were, respectively, 2.0- and 3.1-fold higher than expected. Similar results were obtained when all these fragments were analyzed by HPLC using a TSK-Gel G3000SWxl column equilibrated with the same buffer and pre-calibrated with the same molecular mass standards (Table 1).

The higher apparent molecular masses of the fragments obtained from the size- exclusion chromatography experiments could be connected with homo-interaction between the fragments in solution, i.e. formation of dimers/oligomers. Alternatively, they may reflect abnormal mobility of the fragments due to their nonglobular shape. To select between these alternatives, we tested the aggregation state of these fragments in solution by the multi-angle laser light scattering technique, which offers a shape-independent approach for determination of molecular masses [33]. The apparent molecular masses of the fragments determined from the light scattering data were found to be in a good agreement with those calculated from their amino acid composition (Table 1) suggesting that they are all monomeric in TBS. At the same time, since in these experiments the light scattering was measured immediately after the fragments were eluted from the HPLC column, one could not exclude the possibility that potential interactions between the fragments were disrupted upon size-exclusion chromatography. Therefore, we further tested the aggregation state of the fragments by sedimentation analysis.

In sedimentation velocity experiments, the bAα224-568 fragment and its sub-fragments, bAα224-373 and bAα374-568, each behaved in neutral pH buffer as a single species with sedimentation coefficients ($S_{20,w}$) equal to 2.1, 1.7 and 2.0 S, respectively, as determined by fitting the radial distribution data with SVEDBERG [32]. Analyzing this data by the time-derivative algorithm DCDT+ [31] yielded the distribution of sedimenting species shown in Fig. 4A. The data for the bAα224-568 and bAα224-373 fragments were best described by a single ideal species model, whereas that for bAα374-568 fit better to a two-species model, with a small quantity of material sedimenting at ~6 S (about 7%). For comparison, calculated sedimentation coefficients obtained by treating each fragment as either a hydrated sphere or hydrated random coil with the molecular weight of a monomer are also shown in Fig. 4. Using the full-length bAα224-568 fragment as an example, this calculation yielded 3.4 S for a spherical particle and 1.2 S for a random coil; the experimentally determined value, 2.1 S, fell within these limits. This pattern held for the other two fragments, both

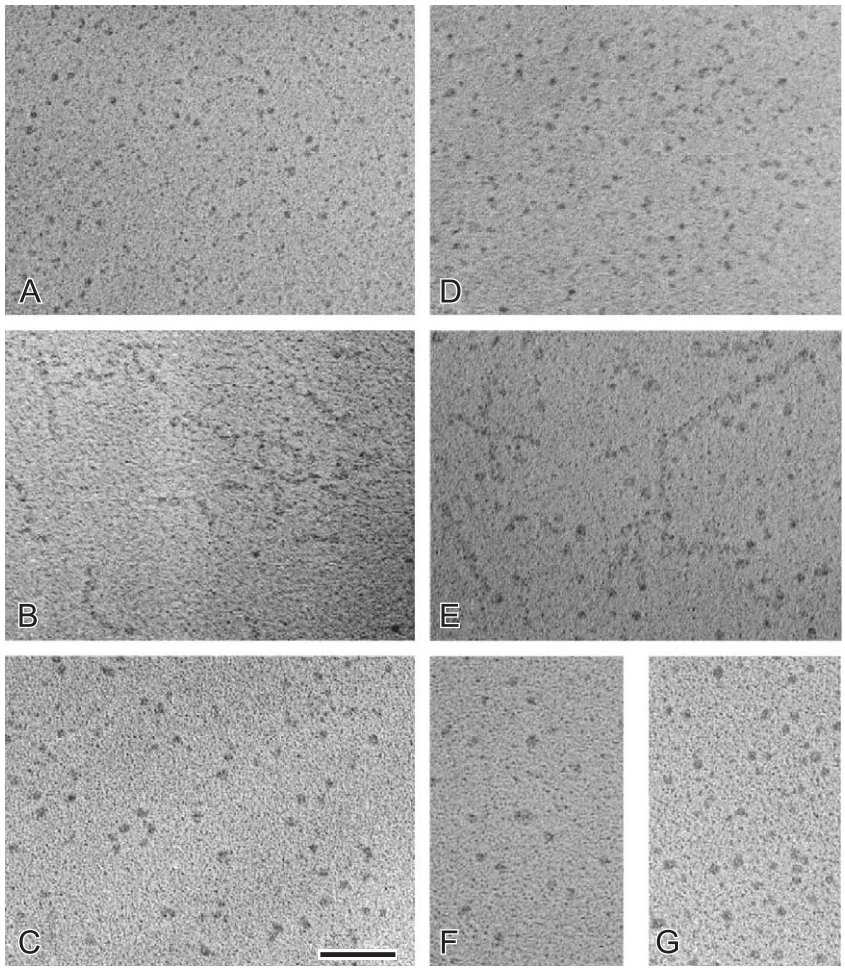

Fig. 3. Electron microscopy of the rotary shadowed samples of the recombinant αC-domain variants. Panels A and B show the bovine bAα224-538 fragment after its transfer from acidic GBS to acidic electron microscopy buffer (0.125% acetic acid, pH 3.5, with 30% glycerol) and neutral pH electron microscopy buffer (20 mM ammonium formate, pH 7.4, with 30% glycerol), respectively, while panel C shows the same fragment after its transfer from neutral pH TBS to the neutral pH electron microscopy buffer. Panels D and E show the bovine bAα224-568 fragment after its transfer from acidic pH GBS to the acidic and neutral pH electron microscopy buffers, respectively, while panel F shows the same fragment after its transfer from neutral pH TBS to the neutral electron microscopy buffer. Panel G shows the human hAα221-610 fragment after its transfer from neutral pH TBS to the neutral pH electron microscopy buffer. Bar for A through G equals 0.1 μM.

of which exhibited sedimentation coefficients within these calculated limits for monomeric species. Similar results were obtained with the recombinant full-length human αC-domain fragment, hAα221-610, and its sub-fragments, hAα221-391 and hAα392-610, which also behaved as single species with $S_{20,w}$ of 2.4, 1.6 and 1.6 S, respectively. Their distributions of sedimenting species are presented in Fig. 4B; in each case, the experimentally determined S values fell within the calculated limits for monomeric species.

These results unambiguously indicate that the recombinant bovine and human αC-domains and their truncated

Table 1
Molecular masses of the recombinant bovine αC-domain variants determined by size-exclusion chromatography and multi-angle light scattering

αC-fragments	M_{calc} (Da)[a]	FPLC		HPLC		Light scattering
		M_{app} (kDa)[b]	M_{app}/M_{calc}	M_{app} (kDa)[b]	M_{app}/M_{calc}	M_w (kDa)[c]
bAα224-568	36,628	99.6±2.3	2.7	98.6±2.5	2.7	34.6±2.2
bAα224-538	33,406	84.9±2.1	2.5	79.2±5.7	2.4	31.7±0.2
bAα224-373	15,433	34.1±3.4	2.0	24.0±3.3	1.6	15.6±0.9
bAα374-568	21,344	65.9±0.1	3.1	64.5±3.3	3.0	21.5±1.4

[a] Molecular masses calculated from amino acid composition of the fragments.
[b] Apparent molecular masses determined by size-exclusion chromatography.
[c] Apparent molecular masses calculated from Zimm plots.

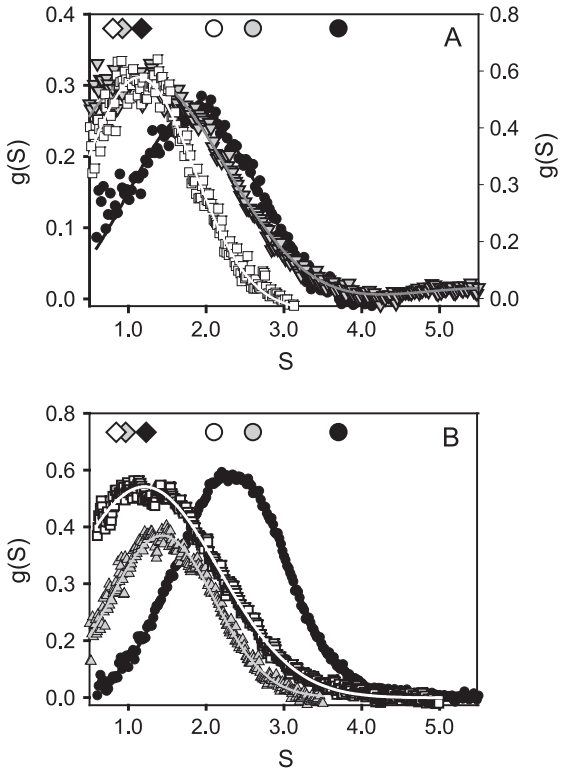

Fig. 4. Distribution of sedimenting species observed with the recombinant bovine (A) and human (B) αC-domains and their truncated variants in TBS. Panel A, data were analyzed with DCDT+ software to obtain plots of weight fraction, $g(s)$ versus sedimentation coefficient(s) as follows: bAα224-568 fragment (black circles), bAα224-373 (white squares) and bAα374-568 (gray triangles). The solid lines were determined by fitting the data with bAα224-568 (black line) and bAα224-373 (white line) to a single species, whereas bAα374-568 was fit to a two-species model with a minor component at ~6 S (gray line). Panel B, data for the human fragments, hAα221-610 (black circles, black line), hAα221-391 (white squares, white line) and hAα392-610 (gray triangles, gray line), were all best described by single species fits. In each panel, the symbols at the top of the figure denote calculated S values for each fragment, based on either spherical, hydrated particles (circles) or random coil, hydrated particles (diamonds). The black, gray, and white symbols follow the same pattern as the experimental data.

variants are essentially all monomeric in TBS. This explains our failure to observe aggregates after dilution of the bAα224-538 and bAα224-568 fragments with neutral pH buffers in experiments mentioned above in Section 3.2. This also suggests that the ordered oligomers observed by EM could be connected either with the rapid change of pH or with the nature of the neutral pH buffer used for preparation of samples for electron microscopy.

3.4. Analysis of the recombinant αC-fragments cross-linked with factor XIIIa

To search further for appropriate models mimicking structural and functional features of the αC-domains in fibrin, we cross-linked the full-length bovine αC-domain fragment, bAα224-568, with factor XIIIa, removed the nonsoluble fraction by centrifugation and further fractionated the soluble cross-linked fraction by size-exclusion chromatography. The fractions containing high molecular mass cross-linked oligomers with mobility slower than the 200-kDa standard (Fig. 5A, lane 2) as well as those containing smaller oligomers, dimers and monomers (Fig. 5A, lanes 3, 4 and 5, respectively) were prepared. Similar results were obtained with the recombinant full-length human fibrinogen αC-domain fragment, hAα221-610 (Fig. 5B). When the first fraction of both cross-linked species was analyzed by EM, oligomers with regular structure were observed in both cases (Fig. 6). There were large oligomers that appeared to be made up of 4 nm globular structures with the same appearance as the individual, unaggregated αC-domains. These structures were often complex, with some regions that were the width of two individual αC-domains and other regions consisting of many branched strands. There were also some smaller oligomers and much larger, more complicated aggregates. The oligomers were reminiscent of those observed after transfer of the bovine αC-domain fragments from acidic to neutral pH [26]. However, these structures observed earlier were simpler in structure, with a width twice that of the individual αC-domain and occasional branch points.

3.5. Adhesion of endothelial cells to the isolated αC-domain and its cross-linked oligomers

To test if oligomerization of the αC-domains changes their functional properties, we compared adhesion of umbilical vein endothelial cells (HUVEC) to the monomeric and FXIIIa-cross-linked oligomeric forms of the recombi-

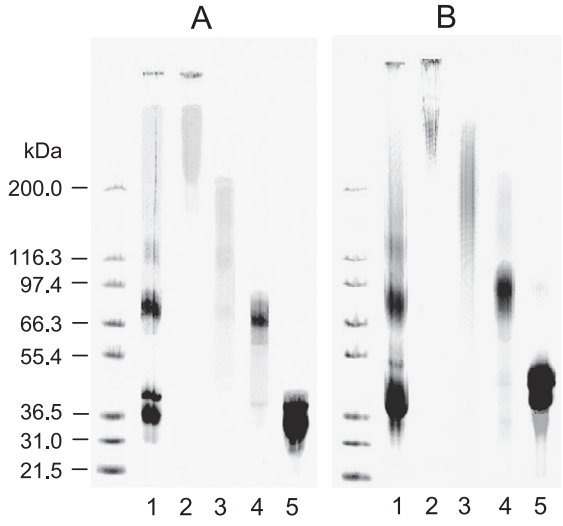

Fig. 5. SDS-PAGE analysis of the factor XIIIa-cross-linked recombinant bovine (panel A) and human (panel B) αC-domain fragments. Lanes 1 in both panels show the soluble portions of the cross-linked fragments, while their individual fractions obtained by size-exclusion chromatography are shown in lanes 2 through 5 (see text). Left outer lanes in both panels contain molecular mass standards.

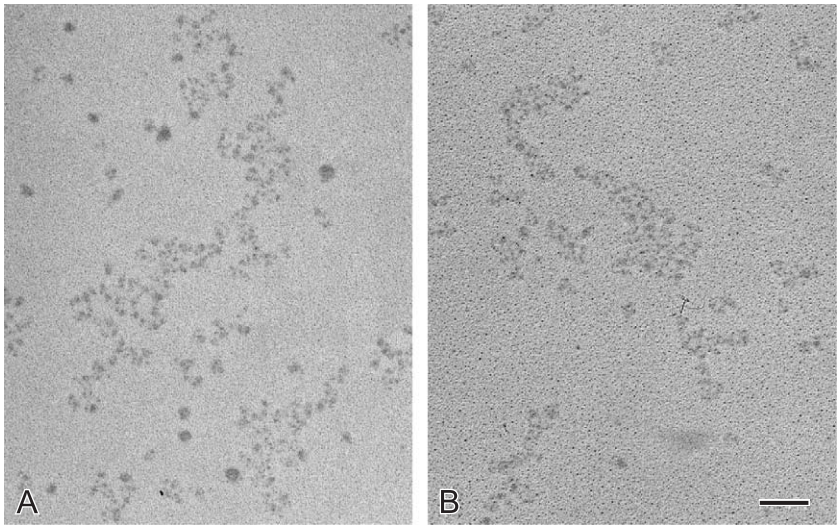

Fig. 6. Electron microscopy of the rotary shadowed samples of the αC-domain fragments cross-linked with factor XIIIa. Panel A shows oligomers observed in the first chromatographic fraction of the cross-linked bovine bAα224-568 fragment while panel B shows similar oligomers observed in the first chromatographic fraction of human hAα221-610 fragment. The SDS-PAGE analysis of these fractions is presented in the previous figure. Bar for A and B equals 0.1 μM.

nant human αC-domains in a static cell adhesion assay. Adhesion of HUVEC to the cross-linked αC-oligomers was increased about 3-fold compared with the adhesion to the non-cross-linked monomers (Fig. 7). In the case of both species, adhesion was reduced to background levels in the presence of the RGD-containing GRGDSP peptide, but not the scrambled GRGESP peptide, indicating a major role of RGD-dependent integrins in the adhesion process. This result indicates that oligomerization of the αC-domains by cross-linking with factor XIIIa substantially increases their cell adhesion properties.

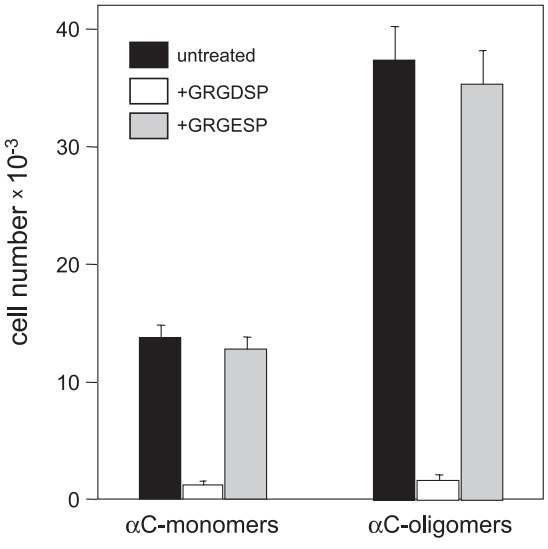

Fig. 7. Adhesion of human umbilical vein endothelial cells (HUVEC) to the immobilized human αC-domain (hAα221-610) and its factor XIIIa-cross-linked oligomers; 10^5 HUVEC cells were plated in serum-free medium for 20 min at 37 °C on plastic wells coated with 20 μg/ml αC-domain monomers or FXIIIa-cross-linked oligomers. Where indicated, 250 μg/ml GRGDSP or GRGESP peptides were added to the wells. Shown are the means of two independent experiments performed in triplicate.

4. Discussion

Fibrinogen is rather inert in the circulation, while fibrin expresses various activities towards different plasma proteins and cell types which contribute to wound healing and other fibrin-dependent physiological and pathological processes. Such reactivity is connected with conformational and other structural changes upon conversion of fibrinogen into fibrin (fibrin assembly) which unmask functionally important cryptic binding sites [34]. Besides the αC-domains, fibrinogen contains multiple domains in its terminal D regions and the central region E. Fibrin assembly occurs mainly through the interactions between complementary polymerization sites located in these regions (DD:E interactions). Conformational changes in the D regions were clarified using a soluble model of fibrin, the fibrin-derived D-D:E_1 complex, which seems to preserve the conformation of fibrin and its major intermolecular interactions [34,35]. The αC-domains, which in fibrin form α polymers, also undergo conformational changes upon fibrin assembly [4]. The structure and function of such polymers remain to be clarified. Previous EM studies revealed that the αC-fragments derived from the fibrinogen αC-domains could form branched oligomers with ordered structure [26]. Since the arrangement and conformation of the αC-domains in such oligomers could mimic those in fibrin, they may represent an appropriate model of fibrin α polymers. In this study, we prepared and characterized soluble oligomers formed by the recombinant αC-domain variants and tested their functional properties.

It is well established that non-cross-linked fibrin polymer can be dissolved in acidic pH buffers, in which it is folded and monomeric, and that after transfer to neutral pH it polymerizes again [1,2,36]. Therefore, in the previous EM study [26], the αC-fragment prepared by plasmin digestion of bovine fibrinogen was also kept at acidic pH prior to transfer to neutral pH buffer, in which it formed ordered oligomers. In this study, we tested the ability of the recombinant analog of this fragment, bAα224-538, as well as the full-length bovine αC-domain, bAα224-568, to form similar oligomers. Since many proteins unfold at acidic pH, we first proved that the recombinant fragments preserved their native folded structure in acidic pH buffer (Fig. 1) and then analyzed their behavior after transfer to neutral pH buffer. Turbidity measurements revealed that both recombinant fragments formed aggregates and EM studies confirmed that the aggregates had an ordered structure (Figs. 2 and 3), indicating that they were formed by specific interactions between binding sites on the αC-domains. These linear polymers had a width of about 8 nm, or twice that of the monomer, and branches were also present. At the same, the analysis of the aggregation state of the fragments kept in neutral pH buffers revealed that all fragments were monomeric suggesting that oligomer formation is connected with the pH change. Nevertheless, we think that these polymers may still be related to the structures formed in fibrin, since one of the main functions of the αC-domains is to self-associate and the specific binding sites are likely to interact under other unique conditions.

In spite of numerous X-ray studies on crystal structure of fibrinogen and its proteolytic and recombinant fragments, the three dimensional structure of the αC-domain has not been established [17,37,38]. One of the possible reasons could be that the αC-domains, which are attached to the bulk of the molecule with the flexible connector, are either missing or are mobile and therefore were not seen on electron density map. This suggests that studies of the isolated αC-domains seem to be a more promising approach to solve their structure. Unfortunately, previous studies on the isolated αC-domains were mainly focused on their cross-linking sites [25,39,40] and functional activities [5,24] because of the reported tendency to form oligomers at neutral pH [26]. We recently expressed bovine and human αC-domain fragments without the connector regions and proved that they are folded into compact structures [22]. In this study, we established by several techniques that these fragments, as well as the other tested variants of the αC-domains, are all monomeric in neutral pH buffers. These two findings provide a basis for crystallization of the compact αC-domain fragments for X-ray analysis and for study of their three dimensional structure by NMR.

Although the oligomers observed after transfer of the αC-fragments from acidic to neutral pH buffer may mimic fibrin α polymers, they seemed to be unstable. Since in fibrin α polymers are stabilized by factor XIIIa, we next cross-linked bovine and human recombinant αC-domains, kept in neutral pH buffer, with factor XIIIa. The cross-linking patterns indicated internal cross-linking as well as the intermolecular ones, similar to those described earlier [25]. The final products containing species of different size were further fractionated and soluble fractions containing species with molecular mass higher than 200 kDa were purified. EM studies revealed that these fractions contained oligomers with ordered structure. These oligomers were similar to those described above, in that many of them are made up of filaments with a width of about 8 nm or twice the diameter of an individual αC nodule, but their structure was more complex and more highly branched (compare Figs. 3 and 5). Again, we think that these polymers reflect aspects of the interactions that occur in cross-linked fibrin. It should be noted that any of the polymers observed would require the presence of at least two pairs of complementary binding sites to form. Furthermore, it is important to remember that the formation of αC-polymers in fibrin will be facilitated and directed by the attachment of the αC-domains to the backbone of the fibrin molecule, so these interactions will be more likely to occur in fibrin in the absence of factor XIIIa cross-linking.

It was shown recently that cross-linking of the human fibrinogen αC-domains with factor XIIIa increases their ability to stimulate activation of plasminogen by tPA [5]. In this study, we found that the cell binding properties of the cross-linked αC-domains are also substantially increased. In fact, in a cell adhesion assay the cross-linked αC-domains supported adhesion of endothelial cells almost 3-fold better than their monomeric counterparts. This study also revealed that the cell adhesion activity of the αC-domains, which contain the RGD sequence, is completely RGD-dependent since it was inhibited by the RGD-containing peptide. This is in agreement with the previous finding that the interaction of fibrin(ogen) with endothelial cells occurs mostly through an RGD-dependent mechanism [14]. Whether the RGD sequences are better exposed in the αC-oligomers or clustering of RGD-containing integrin-binding sites upon oligomerization causes the increased cellular response remains to be established. The cross-linked oligomers prepared in this study are soluble, stable, highly reproducible, and seem to represent an appropriate model to address these questions.

Acknowledgements

This work was supported by National Institute of Health Grants HL-56051 to Leonid Medved, HL30954 to John Weisel, and GM62895 to Alexey Belkin, and by Grant-in-Aid 0355869U from the American Heart Association to Roy Hantgan.

References

[1] L.V. Medved, O.V. Gorkun, V.F. Manyakov, V.A. Belitser, The role of fibrinogen αC-domains in the fibrin assembly process, FEBS Lett. 181 (1985) 109–112.

[2] O.V. Gorkun, Y.I. Veklich, L.V. Medved, A.H. Henschen, J.W. Weisel, Role of the αC domains of fibrin in clot formation, Biochemistry 33 (1994) 6986–6997.

[3] C.S. Cierniewski, A.Z. Budzynski, Involvement of the α chain in fibrin clot formation. Effect of monoclonal antibodies, Biochemistry 31 (1992) 4248–4253.

[4] J.W. Weisel, L. Medved, The structure and function of the αC domains of fibrinogen, Ann. N.Y. Acad. Sci. 936 (2001) 312–327.

[5] G. Tsurupa, L. Medved, Identification and characterization of novel tPA- and plasminogen-binding sites within fibrin(ogen) αC-domains, Biochemistry 40 (2001) 801–808.

[6] Y. Sakata, N. Aoki, Cross-linking of α_2-plasmin inhibitor to fibrin by fibrin-stabilizing factor, J. Clin. Invest. 65 (1980) 290–297.

[7] H.R. Lijnen, J. Soria, C. Soria, D. Collen, J.P. Caen, Dysfibrinogenemia (fibrinogen Dusard) associated with impaired fibrin-enhanced plasminogen activation, Thromb. Haemost. 51 (1984) 108–109.

[8] J. Koopman, F. Haverkate, J. Grimbergen, R. Egbring, S.T. Lord, Fibrinogen Marburg: a homozygous case of dysfibrinogenemia, lacking amino acids Aα 461–610 (Lys 461 AAA→stop TAA), Blood 80 (1992) 1972–1979.

[9] R.B. Credo, C.G. Curtis, L. Lorand, α-chain domain of fibrinogen controls generation of fibrinoligase (coagulation factor XIIIa). Calcium ion regulatory aspects, Biochemistry 20 (1981) 3770–3778.

[10] M.D. Bale, L.G. Westrick, D.F. Mosher, Incorporation of thrombospondin into fibrin clots, J. Biol. Chem. 260 (1985) 7502–7508.

[11] H. Ritchie, L.C. Lawrie, P.W. Crombie, M.W. Mosesson, N.A. Booth, Cross-linking of plasminogen activator inhibitor 2 and α_2-antiplasmin to fibrin(ogen), J. Biol. Chem. 275 (2000) 24915–24920.

[12] M. Hada, M. Kato, S. Ikematsu, M. Fujimaki, K. Fukutake, Possible cross-linking of factor VIII related antigen to fibrin by factor XIII in delayed coagulation process, Thromb. Res. 25 (1982) 163–168.

[13] D.F. Mosher, R.B. Johnson, Specificity of fibronectin–fibrin cross-linking, Ann. N.Y. Acad. Sci. 408 (1983) 583–594.

[14] D.A. Cheresh, S.A. Berliner, V. Vicente, Z.M. Ruggeri, Recognition of distinct adhesive sites on fibrinogen by related integrins on platelets and endothelial cells, Cell 58 (1989) 945–953.

[15] S.A. Corbett, L. Lee, C.L. Wilson, J.E. Schwarzbauer, Covalent cross-linking of fibronectin to fibrin is required for maximal cell adhesion to a fibronectin–fibrin matrix, J. Biol. Chem. 272 (1997) 24999–25005.

[16] S.A. Corbett, J.E. Schwarzbauer, Fibronectin–fibrin cross-linking; a regulator of cell behavior, Trends Cardiovasc. Med. 8 (1998) 357–362.

[17] Z. Yang, J.M. Kollman, L. Pandi, R.F. Doolittle, Crystal structure of native chicken fibrinogen at 2.7 Å resolution, Biochemistry 40 (2001) 12515–12523.

[18] P.L. Privalov, L.V. Medved, Domains in the fibrinogen molecule, J. Mol. Biol. 159 (1982) 665–683.

[19] L.V. Medved, O.V. Gorkun, P.L. Privalov, Structural organization of C-terminal parts of fibrinogen Aα-chains, FEBS Lett. 160 (1983) 291–295.

[20] H.P. Erickson, W.E. Fowler, Electron microscopy of fibrinogen, its plasmic fragments and small polymers, Ann. N.Y. Acad. Sci. 408 (1983) 146–163.

[21] J.W. Weisel, C.V. Stauffacher, E. Bullitt, C. Cohen, A model for fibrinogen: domains and sequence, Science 230 (1985) 1388–1391.

[22] G. Tsurupa, L. Tsonev, L. Medved, Structural organization of the fibrin(ogen) αC-domain, Biochemistry 41 (2002) 6449–6459.

[23] E. Makogonenko, G. Tsurupa, K. Ingham, L. Medved, Interaction of fibrin(ogen) with fibronectin: further characterization and localization of the fibronectin-binding site, Biochemistry 41 (2002) 7907–7913.

[24] G. Tsurupa, B. Ho-Tin-Noe, E. Angles-Cano, L. Medved, Identification and characterization of novel lysine-independent apolipoprotein(a)-binding sites in fibrin(ogen) αC-domains, J. Biol. Chem. 278 (2003) 37154–37159.

[25] Y.V. Matsuka, L.V. Medved, M.M. Migliorini, K.C. Ingham, Factor XIIIa-catalyzed cross-linking of recombinant αC fragments of human fibrinogen, Biochemistry 35 (1996) 5810–5816.

[26] Y.I. Veklich, O.V. Gorkun, L.V. Medved, W. Nieuwenhuizen, J.W. Weisel, Carboxyl-terminal portions of the α chains of fibrinogen and fibrin. Localization by electron microscopy and the effects of isolated αC fragments on polymerization, J. Biol. Chem. 268 (1993) 13577–13585.

[27] S. Rudchenko, I. Trakht, J.H. Sobel, Comparative structural and functional features of the human fibrinogen αC domain and the isolated αC fragment. Characterization using monoclonal antibodies to defined COOH-terminal Aα chain regions, J. Biol. Chem. 271 (1996) 2523–2530.

[28] J. Wen, T. Arakawa, J.S. Philo, Size-exclusion chromatography with on-line light-scattering, absorbance, and refractive index detectors for studying proteins and their interactions, Anal. Biochem. 240 (1996) 155–166.

[29] R.R. Hantgan, C. Paumi, M. Rocco, J.W. Weisel, Effects of ligand-mimetic peptides Arg–Gly–Asp–X (X=Phe, Trp, Ser) on αIIbβ3 integrin conformation and oligomerization, Biochemistry 38 (1999) 14461–14474.

[30] R.R. Hantgan, M. Rocco, C. Nagaswami, J.W. Weisel, Binding of a fibrinogen mimetic stabilizes integrin αIIbβ3's open conformation, Protein Sci. 10 (2001) 1614–1626.

[31] W.F. Stafford III, Boundary analysis in sedimentation transport experiments: a procedure for obtaining sedimentation coefficient distributions using the time derivative of the concentration profile, Anal. Biochem. 203 (1992) 295–301.

[32] T.M. Laue, B.D. Shah, T.M. Ridgeway, S. Pelletier, in: S.E. Harding, A.J. Rowe, J.C. Horton (Eds.), Analytical Ultracentrifugation in Biochemistry and Polymer Science, The Royal Society of Chemistry, Cambridge, 1992, pp. 90–125.

[33] P.J. Wyatt, Combined differential light scattering with various liquid chromatography separation techniques, Biochem. Soc. Trans. 19 (1991) 485–486.

[34] L. Medved, G. Tsurupa, S. Yakovlev, Conformational changes upon conversion of fibrinogen into fibrin. The mechanism of exposure of cryptic sites, Ann. N.Y. Acad. Sci. 408 (1983) 185–204.

[35] S. Yakovlev, E. Makogonenko, N. Kurochkina, W. Nieuwenhuizen, K. Ingham, L. Medved, Conversion of fibrinogen to fibrin: mechanism of exposure of tPA- and plasminogen-binding sites, Biochemistry 39 (2000) 15730–15741.

[36] V.A. Belitser, T.V. Varetskaja, G.V. Malneva, Fibrinogen–fibrin interaction, Biochim. Biophys. Acta 154 (1968) 367–375.

[37] J.H. Brown, N. Volkmann, G. Jun, A.H. Henschen-Edman, C. Cohen, The crystal structure of modified bovine fibrinogen, Proc. Natl. Acad. Sci. U. S. A. 97 (2001) 85–90.

[38] R.F. Doolittle, X-ray crystallographic studies on fibrinogen and fibrin, Thromb. Haemost. 1 (2003) 1559–1565.

[39] Y.V. Matsuka, M.M. Migliorini, K.C. Ingham, Cross-linking of fibronectin to C-terminal fragments of the fibrinogen α-chain by factor XIIIa, J. Protein Chem. 16 (1997) 739–745.

[40] J.H. Sobel, M.A. Gawinowicz, Identification of the α chain lysine donor sites involved in factor XIIIa fibrin cross-linking, J. Biol. Chem. 271 (1996) 12297–19288.